

Date of publication xxxx 00, 0000, date of current version xxxx 00, 0000.

Digital Object Identifier 10.1109/ACCESS.2017.DOI

# Identification of Partial Shading Conditions for Photovoltaic Strings

ZIQUIANG BI<sup>1,2</sup>, (Student Member, IEEE), JIEMING MA<sup>1</sup>, (Member, IEEE), KANGSHI WANG<sup>1</sup>, KA LOK MAN<sup>1,3,4</sup>, JEREMY S. SMITH<sup>2</sup> and YONG YUE<sup>1</sup>

<sup>1</sup>Department of Computer Science and Software Engineering, Xi'an Jiaotong-Liverpool University, Suzhou, 215123, China (e-mail: {Ziqiang.Bi, Ka.Man, Yong.Yue}@xjtlu.edu.cn, Kangshi.Wang@liverpool.ac.uk)

<sup>2</sup>Department of Electrical Engineering and Electronics, University of Liverpool, Liverpool, L69 3GJ, United Kingdom (e-mail: J.S.Smith@liverpool.ac.uk)

<sup>3</sup>imec-DistriNet, KU Leuven, Leuven, B-3001, Belgium

<sup>4</sup>Faculty of Engineering, Computing and Science, Swinburne University of Technology Sarawak Campus, Kuching 93350, Malaysia

Corresponding author: Jieming Ma (e-mail: Jieming.Ma@xjtlu.edu.cn).

This work was supported by the National Natural Science Foundation of China (Grant No. 61702353), the Suzhou Science and Technology Project-Key Industrial Technology Innovation (Grant No. SYG201841), Qing Lan Project of Jiangsu Province, the Open Foundation of the Suzhou Smart City Research Institute, Suzhou University of Science and Technology, the Key Program Special Fund of Xi'an Jiaotong-Liverpool University (XJTLU), Suzhou, China (Grant No. KSF-P-02, KSF-E-65), and the Research Development Fund of XJTLU (Grant No. RDF-14-02-32, RDF-17-02-04).

**ABSTRACT** Under partial shading conditions (PSC), the power-voltage (P-V) characteristic curve of photovoltaic (PV) strings exhibits multiple peaks. Such mismatching phenomenon brings challenges in controlling the output power. To analyze the electrical characteristics of PV strings in complex environments, a quantitative analysis method is required to characterize the PSC. This paper introduces the shading matrix to describe the shading rate and shading strength information. The proposed shading matrix would provide maximum power point tracking (MPPT) controllers with the essential environmental information to improve the global maximum power point (GMPP) tracking performance. A modified Tabu search (MTS) based identification method is proposed to estimate the shading matrix. The proposed modified method involves a preselection process of updating the Tabu list to optimize the searching efficiency. The accuracy and efficiency of the proposed analytical estimation expression are validated through simulations and experiments. By comparing with binary search (BS), golden-section search (GS) and Tabu search (TS) algorithms, the proposed MTS algorithm is demonstrated to perceive the shading information at least 18.75% faster.

**INDEX TERMS** Shading matrix, partial shading conditions, photovoltaic cells, solar energy, Tabu search.

## I. INTRODUCTION

IN photovoltaic (PV) systems, PV modules are usually connected in series or parallel to form a PV string or array in order to generate sufficient power. The series-connected PV string is the prior configuration of PV modules in terms of the lowest mismatch power losses due to the non-uniform irradiance [1]. When the PV modules in a PV string receive non-uniform solar irradiations, the string is considered to operate under partial shading conditions (PSC). The shaded PV modules would be easily damaged under PSC without any protection due to the "hot-spot" effect [2]. As a result, bypass diodes are normally connected to the PV modules [3]. However, with the existence of the bypass diodes, the current-voltage (I-V) characteristic curves exhibit multiple stairs with turning points [4]–[6] and correspondingly, the power-voltage (P-V) characteristic curves of the PV string,

under PSC, exhibit multiple peaks [7]. That brings difficulties in controlling and optimizing the output string power. A quantitative analysis of PSC would provide necessary information for the power management systems.

In the recent years, many fault diagnosis methods have been proposed to detect or distinguish the partial shading in PV systems from the uniform irradiation conditions (UIC). A diagnosis method based on characteristics deviation analyses was presented in [8]. It indicates that the PSC can be distinguished by observing the stairs in I-V characteristic curves. This method cannot detect the PSC automatically since manual observations are required. In [9], an artificial neural network (ANN) is used to detect the faults under normal and partially shaded conditions. The ANN-based fault diagnosis method is capable of distinguishing the PSC from UIC automatically by inputting the solar radiation, tem-

**Nomenclature**

$\alpha_i$	the fractional factor of $V_{OC,Module}$	$L_T$	the terminated length of the interval (V)
$\Delta G_{tolerance}$	the tolerated solar irradiance ( $W/m^2$ )	$M_S$	the shading matrix
$\Delta I_{ref}$	the reference current difference (A)	$n$	the ideality factor of the diode
$D_{new}$	the slope of the newly sampled point (A/V)	$N_{String}$	the number of modules in the PV string
$D_{ref}$	the reference slope (A/V)	$P_{MPP}$	the power at the maximum power point (W)
$G$	the actual solar irradiance ( $W/m^2$ )	$q$	the electron charge (C)
$G_{STC}$	the reference irradiance at standard test conditions ( $W/m^2$ )	$R_{sh}$	the shunt resistance ( $\Omega$ )
$I_{lb}$	the left boundary of the initial candidate interval (A)	$R_s$	the series resistance ( $\Omega$ )
$I_{MPP}$	the current at the maximum power point (A)	$T$	the ambient temperature (K)
$I_{new}$	the current of the newly sampled point (A)	$T_{STC}$	the reference temperature at standard test conditions (K)
$I_{ph}$	the light-generated photocurrent (A)	$V_{MPP}$	the voltage at the maximum power point (V)
$I_{PV}$	the operating current of the PV string (A)	$V_{PV}$	the operating voltage of the PV string (V)
$I_{rb}$	the right boundary of the initial candidate interval (A)	$\chi_i$	the $i$ th shading rate information
$I_{ref}$	the reference current in the judging criterion (A)	$\rho_i$	the $i$ th shading strength information
$I_{sat}$	the reverse saturation current (A)	$G_{Insolated}$	the solar irradiance of the insolated PV modules ( $W/m^2$ )
$I_{SC,Insolated}$	the short-circuit current of the insolated modules (A)	$G_{Shaded,i}$	the $i$ th shaded irradiance ( $W/m^2$ )
$I_{SC,Shaded,i}$	the $i$ th shaded short-circuit current (A)	$N_{Series}$	the number of series cells in the PV module
$I_{SC,STC}$	the reference short-circuit current at standard test conditions (A)	$N_{Shaded,i}$	the number of shaded modules under the $i$ th shaded irradiance
$I_{SC,String}$	the string short-circuit current (A)	$N_{Shaded}$	the number of shaded modules
$I_{SC}$	the short-circuit current (A)	$N_i$	the number of shaded modules with the irradiation not higher than $G_{Shaded,i}$
$I_{TP,i}$	the current at the $i$ th turning point (A)	$V_{BD}$	the breakdown voltage of the shaded modules (V)
$k$	the Boltzmann's constant (eV/K)	$V_{Insolated}$	the voltage of the insolated modules (V)
$K_I$	the short-circuit current temperature co-efficient (A/K)	$V_{OC,Module}$	the open-circuit voltage of the individual PV module (V)
$K_V$	the open-circuit voltage temperature co-efficient (V/K)	$V_{OC,String}$	the open-circuit voltage of the PV string (V)
		$V_{Shaded}$	the voltage of the shaded modules (V)
		$V_{TP,i}$	the voltage at the $i$ th turning point (V)
		$V_{TP}$	the voltage at the turning point (V)

perature and measured output power. Zhao et al. proposed a novel PV array fault diagnosis method based on fuzzy C-mean (FCM) and fuzzy membership algorithms in [10]. It uses clustering to analyze different PV faults under both UIC and PSC. By comparing with the K-means, the running time of the FCM algorithm is longer but the accuracy is higher. In [11], a fault diagnostic technique for PV systems based on measured I-V characteristics was proposed. The partial shading faults can be distinguished by a multi-class adaptive boosting (AdaBoost) from some other PV faults such as the short-circuit and abnormal aging. Principal component analysis (PCA) was applied to identify the shading in PV systems using the features from I-V characteristic curves in [12]. This method only uses the PV current and voltage, which avoids additional hardware and costs. However, these fault diagnosis systems can only detect the existence of PSC. The detailed shading conditions cannot be identified.

In order to analyze PSC, the shading information has been proposed in the recent ten years [13]. Typically, the shading information refers to the shading rate and shading strength [14]. The shading rate represents the percentage of the shaded PV modules in the PV string [14]. The shading strength reflects the ratio of the solar irradiance of the PV modules in the PV string [15]. Different combinations of the shading rate and shading strength will result in varied PV characteristics. Early studies have shown that these two shading factors directly influence the locus of the global maximum power point (GMPP) [16], [17]. Many shading information detection methods have been proposed. An automatic shading detection method by using voltage sensors and a switch matrix was proposed in [18]. The detection system has the ability to estimate the shading rate effectively. An ANN is used in [15] to detect the shading information including both the shading rate and shading strength but

this method uses separate ANN models to predict different shading information. In [14], a shading detection method was proposed to predict the shading rate by a sorting algorithm. After determining the shading rate, the shading strength is estimated by multi-output support vector regression (M-SVR). However, this detection method uses the expensive solar irradiance sensors and also carries heavy computational burdens. Some researches have shown that the values of the shading information are related to the location of the turning point in the I-V curves [4], [5]. The number of shaded modules is estimated through the voltage at the turning point in [19]. The shading rate can be further estimated by this identification method. Lei et al. interpreted the PV characteristics under PSC via an analytical model [20]. The shading strength variation is shown to be well correlated to the height of the current steps (turning points) in the I-V characteristics. In [5], the discrete wavelet transform (DWT) is used to interpret the traced I-V curve of the PV system and locate the turning points. However, the definitions of the aforementioned shading information are based on a strong assumption that the PSC only has two irradiation levels.

This paper proposes a comprehensive shading identification approach. The shading matrix is introduced to quantitatively analyze the PSC with multiple irradiation levels. A modified Tabu search (MTS) based identification method is proposed to estimate the shading matrix from the located turning points. The proposed method would provide maximum power point tracking (MPPT) controllers with the essential environmental information to improve the GMPP tracking performance.

The rest of the paper is organized as follows: Section II analyzes the PV characteristics by a mathematical model and introduces the shading matrix for PSC. The methodologies of the identification method for the shading matrix are shown in Section III. The simulation and experimental results are demonstrated in Section IV to validate the accuracy and efficiency of the proposed identification method. Section V presents the conclusions of this paper.

## II. ELECTRICAL CHARACTERISTICS OF A PHOTOVOLTAIC STRING

### A. PHOTOVOLTAIC CHARACTERISTICS UNDER UNIFORM IRRADIATION CONDITIONS

The I-V characteristics of a PV string under UIC can be expressed by a single-diode model as shown in (1) [21]–[23].

$$I_{PV} = I_{ph} - I_{sat} \left\{ \exp \left[ \frac{q(V_{PV} + I_{PV}R_s)}{nkTN_s} \right] - 1 \right\} - \frac{V_{PV} + I_{PV}R_s}{R_{sh}} \quad (1)$$

where  $I_{PV}$  and  $V_{PV}$  are the current and voltage of the PV string, respectively;  $I_{ph}$  the light-generated photocurrent;  $I_{sat}$  the reverse saturation current;  $R_s$  the series resistance;  $R_{sh}$  the shunt resistance;  $n$  the ideality factor of the diode;  $N_s = N_{String} \times N_{Series}$  ( $N_{String}$  the number of modules in the PV string and  $N_{Series}$  the number of series cells in the PV module);  $q$  the electron charge;  $k$  the Boltzmann's constant

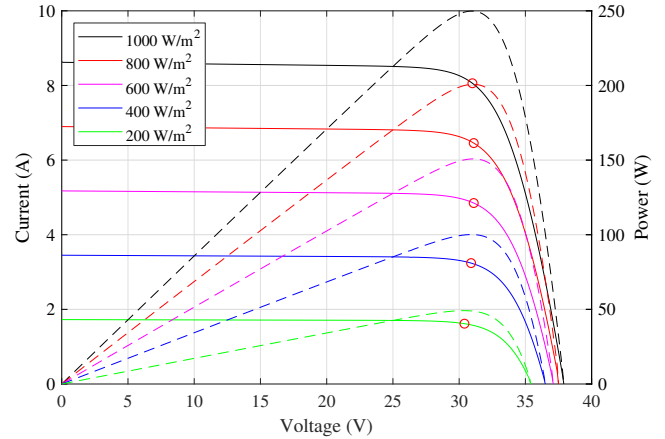


FIGURE 1. Electrical characteristics of a PV string under uniform irradiation conditions (UIC).

and  $T$  the temperature in Kelvin. As the shunt resistance  $R_{sh}$  is relatively large in the majority of the PV modules, the terms related to  $R_{sh}$  can be omitted [24] and (1) can be further simplified to (2).

$$I_{PV} = I_{ph} - I_{sat} \left\{ \exp \left[ \frac{q(V_{PV} + I_{PV}R_s)}{nkTN_s} \right] - 1 \right\} \quad (2)$$

Thus, based on (2), the current slope with respect to the voltage  $dI_{PV}/dV_{PV}$  can be calculated by (3).

$$\frac{dI_{PV}}{dV_{PV}} = -I_{sat} \frac{q}{nkTN_s} \left( 1 + \frac{dI_{PV}}{dV_{PV}} R_s \right) \exp \left[ \frac{q(V_{PV} + I_{PV}R_s)}{nkTN_s} \right] \quad (3)$$

By solving (3), the value of  $dI_{PV}/dV_{PV}$  can be obtained as given in (4).

$$\frac{dI_{PV}}{dV_{PV}} = -1 / \left\{ \frac{nkTN_s}{qI_{sat} \exp[q(V_{PV} + I_{PV}R_s)/(nkTN_s)]} + R_s \right\} \quad (4)$$

FIGURE 1 shows the I-V and P-V characteristics of a PV string under UIC with varied solar irradiances. The maximum power points (MPPs) are marked with the red circles on the I-V curves. As can be found from FIGURE 1, the slope of the I-V curve before the MPP is relatively flat and the slope after the MPP is high. Therefore, in this paper, the slope at the MPP is defined as a reference slope  $D_{ref}$  to distinguish the points with low slopes and points with high slopes.  $D_{ref}$  can be expressed by (5).

$$\begin{aligned} D_{ref} &= \frac{dI_{MPP}}{dV_{MPP}} \\ &= -1 / \left\{ \frac{nkTN_s}{qI_{sat} \exp[q(V_{MPP} + I_{MPP}R_s)/(nkTN_s)]} + R_s \right\} \end{aligned} \quad (5)$$

where  $V_{MPP}$  and  $I_{MPP}$  are respectively the voltage and current at the MPP.

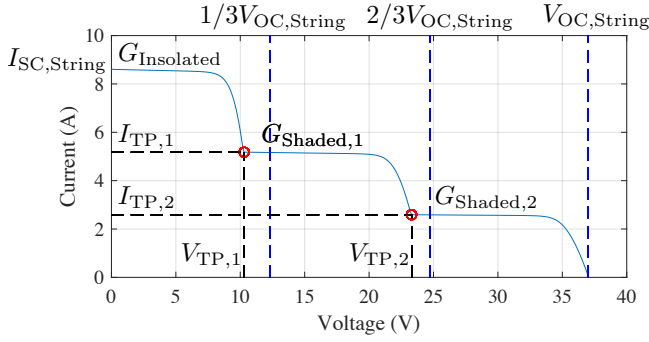


**FIGURE 2.** I-V characteristics of a PV string under partial shading conditions (PSC).

### B. PARTIAL SHADING CONDITIONS AND SHADING MATRIX

FIGURE 2 shows the I-V characteristics of a PV string with three modules. The PV string is operating under the PSC with three individual irradiation levels. Two turning points are exhibited on the I-V curve, which are marked with the red circles. For a PV string with  $N_{String}$  modules, the I-V curve is divided into  $N_{String}$  adjacent intervals with the same length. The boundaries of the intervals are at the integer multiples of  $V_{OC,String}/N_{String}$  and marked by the blue vertical dashed lines in FIGURE 2. Each interval has at most one turning point. Assume that one turning point at  $V_{TP}$  is located in the  $m$ th interval, then the range of  $V_{TP}$  can be obtained as given in (6).

$$(m - 1) \frac{V_{OC,String}}{N_{String}} < V_{TP} < m \frac{V_{OC,String}}{N_{String}} \quad (6)$$

where  $V_{OC,String}$  is the open-circuit voltage of the PV string. Multiplied by  $N_{String}/V_{OC,String}$  on all sides of (6), it can be rewritten as in (7).

$$m - 1 < \frac{N_{String}}{V_{OC,String}} V_{TP} < m \quad (7)$$

The  $m$  can be rounded upwards to the nearest integer as shown in (8).

$$m = \text{ceil}\left(\frac{N_{String}}{V_{OC,String}} V_{TP}\right) \quad (8)$$

where  $\text{ceil}(\cdot)$  is a function that rounds the number to the nearest following integer. The boundary voltage of the interval where the turning points are located can be calculated from the voltage at the turning points.

The shading matrix is the combination of the shading rate and shading strength information. The shading matrix  $M_S$  is expressed by (9).

$$M_S = \begin{bmatrix} \rho_1 & \chi_1 \\ \rho_2 & \chi_2 \\ \vdots & \vdots \\ \rho_{M-1} & \chi_{M-1} \end{bmatrix} \quad (9)$$

where  $M$  is the number of the irradiation levels;  $\rho_i$  and  $\chi_i$

are respectively the  $i$ th shading strength information and the corresponding shading rate information as shown in (10) and (11).

$$\rho_i = \frac{G_{Shaded,i}}{G_{Insolated}} \quad (10)$$

where  $G_{Shaded,i}$  is the  $i$ th shaded irradiance and  $G_{Insolated}$  is the solar irradiance of the insolated PV modules.

$$\chi_i = \frac{N_{Shaded,i}}{N_{String}} \quad (11)$$

where  $N_{Shaded,i}$  is the number of shaded modules under the  $i$ th shaded irradiance.

For a PV string with  $M$  irradiation levels, the dimension of the corresponding shading matrix is  $(M - 1) \times 2$ . Each turning point in the I-V characteristic curve represents a row of the shading matrix. Each row of the shading matrix is a pair of shading rate and strength information. These  $M - 1$  pairs of shading information form the shading matrix.

### III. PROPOSED IDENTIFICATION METHOD

The proposed shading matrix identification method is composed of two stages. In the first stage, the searching method based on a modified Tabu search (MTS) algorithm is used to locate the position of the turning points. In the second stage, the analytical expressions are adopted to estimate the value of the shading matrix.

#### A. LOCATING TURNING POINTS BY A MODIFIED TABU SEARCH ALGORITHM

Turning points are the crucial operating points in I-V characteristic curves of a PV string. The mismatches among the PV cells in the PV string under PSC will result in the existence of the turning points, whose locations reflect the values of the shading information.

The Tabu search (TS) algorithm is a metaheuristic search method employing local search methods used for global mathematical optimization [25], [26]. Inspired by the idea of Tabu lists in the TS algorithm, a modified TS-based method is proposed to search for the turning points in the I-V curve. The proposed method preselects the Tabu lists based on the I-V characteristics to optimize the searching efficiency.

In the preselection process, the Tabu list records the intervals that do not contain turning points. With the establishment of the Tabu list, the proposed identification system only searches the intervals containing turning points and skips the unnecessary intervals, accelerating the searching process. The intervals that may contain the turning points are called candidate intervals. A candidate list is introduced to record the candidate intervals. The Tabu list and candidate list are two opposite lists. These two lists are updated iteratively according to a judging criterion until the termination condition is satisfied.

The pseudocode of the MTS-based searching method is given in Algorithm 1. It consists of two main procedures including the preselection stage and the judging stage.

**Algorithm 1** The turning point searching method based on an MTS algorithm

**Input:** the terminated smallest interval length  $L_T$ , the reference slope  $D_{ref}$  by (5), the reference current difference  $\Delta I_{ref}$  by (15)

**Output:** the location of the turning points

```

%% Preselection Stage
1: Measure  $I_{SC,String}$  and  $V_{OC,String}$ .
2: Divide the I-V characteristic curve into  $N_{String}$  adjacent  $V_{OC,String}/N_{String}$  intervals from 0 to  $V_{OC,String}$ .
3: Tabu list  $\leftarrow$  the last  $V_{OC,String}/N_{String}$  interval.
4: for interval in the rest  $V_{OC,String}/N_{String}$  intervals do
5:   Measure the current difference between the interval boundaries  $\Delta I$ .
6:   if  $\Delta I \leq \Delta I_{ref}$  then
7:     Tabu list  $\leftarrow$  interval.
8:   else
9:     candidate list  $\leftarrow$  interval.
10:  end if
11: end for
%% Judging Stage
12: for candidate interval in candidate list do
13:   Obtain the reference current  $I_{ref}$  by (16).
14:   while the length of candidate interval is greater than  $L_T$  do
15:     Randomly sample a new point in interval.
16:     if  $D_{new} > D_{ref}$  &&  $I_{new} < I_{ref}$  then
17:       Tabu list  $\leftarrow$  the interval right of the new point.
18:     else
19:       Tabu list  $\leftarrow$  the interval left of the new point.
20:     end if
21:     Reduce the candidate interval by Tabu list.
22:   end while
23:   Record the  $V_{TP}$  in the candidate interval as the right boundary. Measure the current at the turning point.
24: end for

```

### 1) Preselection Stage

At the beginning,  $V_{OC,String}$  and  $I_{SC,String}$  are measured. The I-V curve is divided into several intervals with an interval length of  $V_{OC,String}/N_{String}$  according to the finding that each  $V_{OC,String}/N_{String}$  interval contains at most one turning point.

FIGURE 3(a) is a typical example of an I-V characteristics curve from a PV string with three modules under PSC. The I-V curve is divided into three intervals. With the observation that the turning points cannot exist in the last  $V_{OC,String}/N_{String}$  interval, the last  $V_{OC,String}/N_{String}$  interval is recorded in the Tabu list. The intervals in the Tabu list are marked by a shadow as shown in FIGURE 3(a).

For the remaining intervals in the candidates, an initial selection rule will be applied. As shown in FIGURE 3(b) and 3(c), for each initial candidate interval, the current difference

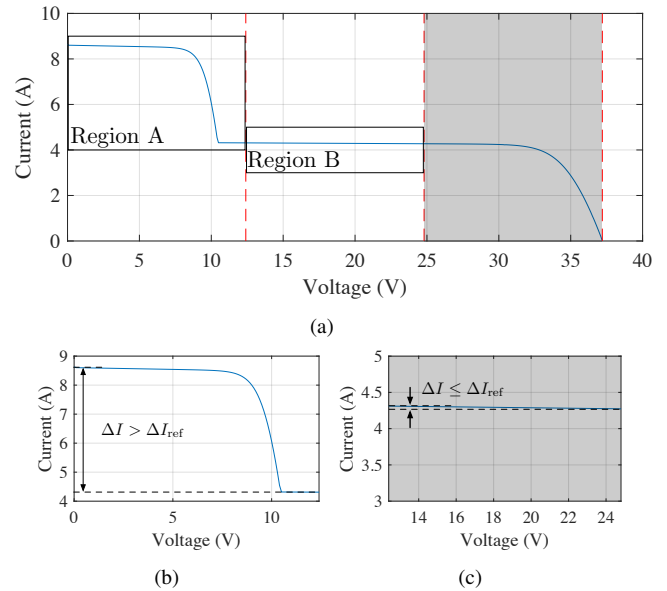


**FIGURE 3.** Initial selection rule for the Tabu List: (a) overall I-V curve; (b) region A; (c) region B.

across the whole interval  $\Delta I$  is measured and compared with a reference value  $\Delta I_{ref}$ . If  $\Delta I > \Delta I_{ref}$ , as shown in FIGURE 3(b), then the current interval is considered as a candidate interval. Otherwise, as shown in FIGURE 3(c), the interval is listed in the Tabu list.

The determination of the reference current difference  $\Delta I_{ref}$  is calculated as follows. The current difference between the boundaries of the  $V_{OC,String}/N_{String}$  interval  $\Delta I$  can be considered as the difference of two short-circuit currents as shown in (12) assuming that the temperature does not change during the two current sampling processes.

$$\Delta I = \Delta I_{SC} \quad (12)$$

Since the short-circuit current  $I_{SC}$  can be modeled by (13) [22], (12) can be extended to (14)

$$I_{SC} = (I_{SC,STC} + K_1 \Delta T) \frac{G}{G_{STC}} \quad (13)$$

where  $I_{SC,STC}$  is the reference short-circuit current at standard test conditions (STC, 25 °C and 1000 W/m<sup>2</sup>);  $K_1$  the short-circuit current temperature co-efficient;  $\Delta T = T - T_{STC}$  the temperature difference between the actual temperature and the reference temperature at STC;  $G$  the actual solar irradiance and  $G_{STC}$  the reference irradiance at STC.  $I_{SC,STC}$  and  $K_1$  can be found in the datasheet of the PV modules.

$$\Delta I = \Delta I_{SC} = [I_{SC,STC} + K_1(T - T_{STC})] \frac{\Delta G}{G_{STC}} \quad (14)$$

Therefore,  $\Delta I_{ref}$  can be expressed by (15).

$$\Delta I_{ref} = [I_{SC,STC} + K_1(T - T_{STC})] \frac{\Delta G_{tolerance}}{G_{STC}} \quad (15)$$

where  $\Delta G_{\text{tolerance}}$  is the tolerated solar irradiance, which means that below this reference value, two irradiation levels are considered as the same level. In this research, the  $\Delta G_{\text{tolerance}}$  is set to  $50 \text{ W/m}^2$ . Hence,  $\Delta I_{\text{ref}} = 0.05 \times [I_{\text{sc,STC}} + K_1(T - 298.15)]$ .

## 2) Judging Stage

In the preselection stage, the intervals containing the turning points are selected. Afterwards, for each candidate intervals, new sampling points are iteratively and randomly selected to reduce the intervals. A judging criterion is introduced to update the Tabu list and the candidate list. FIGURE 4 shows the judging criterion for three major cases. For each  $V_{\text{OC,String}}/N_{\text{String}}$  interval in the candidate list, a reference current  $I_{\text{ref}}$  is defined as the mean value of two boundary currents and can be expressed by (16).  $I_{\text{ref}}$  is represented as the red horizontal dashed lines in FIGURE 4(a) and 4(b).

$$I_{\text{ref}} = \frac{1}{2}(I_{\text{lb}} + I_{\text{rb}}) \quad (16)$$

where  $I_{\text{lb}}$  and  $I_{\text{rb}}$  are respectively current at the left and right boundaries of the initial candidate interval.

A reference slope  $D_{\text{ref}}$  is set by (5) to distinguish if the newly sampled point is in the flat region or steep region. Totally there are three cases, as follows, for the position of the newly sampled point.

When the slope of the newly sampled point  $D_{\text{new}}$  is larger than  $D_{\text{ref}}$ , the new point is sampled on the flat region. As shown in FIGURE 4(a) and 4(b), there are two different cases. The current of the newly sampled point is measured as  $I_{\text{new}}$ . If  $I_{\text{new}} > I_{\text{ref}}$  as shown in FIGURE 4(a), the new point is on the higher flat region and the turning point is to the right of the point as a result, the interval left of the point is added to the Tabu list. Otherwise, the right interval is added to the Tabu list as shown in FIGURE 4(b).

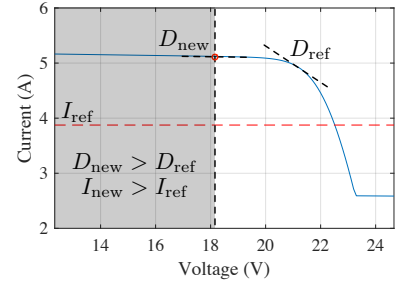
When  $D_{\text{new}} \leq D_{\text{ref}}$  as shown in FIGURE 4(c), the new point is located on the steep slope. The position of the turning point is to the right of the current point. Therefore, the Tabu list is updated by adding the interval left of the point.

This judging rule is used to reduce each candidate interval until the termination condition is satisfied. The termination condition is that the length of the interval is not larger than the selected threshold  $L_T$ . The value of the  $L_T$  will affect the accuracy of the searched turning points. A smaller  $L_T$  can find the turning points more accurately but the searching time is longer and vice versa.

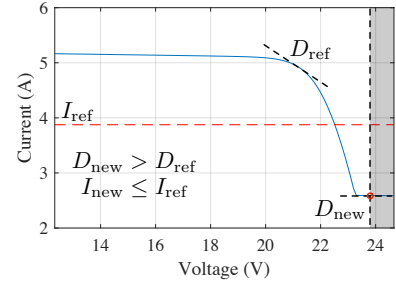
When the termination condition is satisfied, the voltage at the right boundary of the reduced candidate interval is used as the voltage of the turning point in this interval. The current at the turning point can be obtained when the voltage is known.

## B. ANALYTICAL EXPRESSIONS FOR SHADING MATRIX

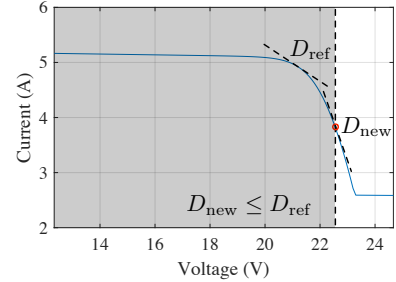
In order to have an easier analysis of the relationship between the shading matrix and the positions of the turning points, the situation with only two solar irradiance levels (one turning point) is investigated. FIGURE 5 depicts the relationships



(a)



(b)



(c)

**FIGURE 4.** The judging criterion for three different cases: (a) case 1:  $D_{\text{new}} > D_{\text{ref}}$ ,  $I_{\text{new}} > I_{\text{ref}}$ ; (b) case 2:  $D_{\text{new}} > D_{\text{ref}}$ ,  $I_{\text{new}} \leq I_{\text{ref}}$ ; (c) case 3:  $D_{\text{new}} \leq D_{\text{ref}}$ .

between the shading information and the position of the turning point under various shading patterns. As can be seen from FIGURE 5(b) and 5(d), the value of the shading rate information is linearly proportional to the voltage at the turning point while the shading strength information has a linear relation with the current at the turning point. With these findings, the shading matrix under the PSC with multiple irradiation levels can be estimated by the located turning points.

### 1) Estimating the Shading Rate Information

As shown in (17), the operating voltage  $V_{\text{PV}}$  of the PV string equals the sum of the voltages from the insolated modules and the voltages from the shaded modules [19].

$$V_{\text{PV}} = (N_{\text{String}} - N_{\text{Shaded}})V_{\text{Insolated}} + N_{\text{Shaded}}V_{\text{Shaded}} \quad (17)$$

where  $N_{\text{Shaded}}$  is the number of shaded modules;  $V_{\text{Insolated}}$  and  $V_{\text{Shaded}}$  are respectively the voltage of the insolated modules and shaded modules.

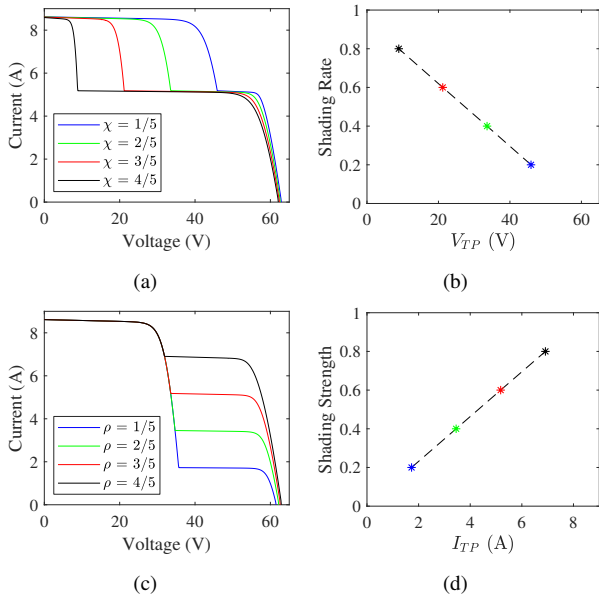


**FIGURE 5.** Relationships between the shading information and the position of the turning point for a PV string with five PV modules. (a) I-V curves with different shading rate information; (b) the relationship between the shading rate information and the voltage at the turning point  $V_{TP}$ ; (c) I-V curves with different shading strength information; (d) the relationship between the shading strength information and the current at the turning point  $I_{TP}$ .

When operating at the  $i$ th turning point  $V_{TP,i}$ , the shaded modules are at the reverse breakdown point because of the bypass diodes. In [19], the voltage of the insulated modules is assumed to be the  $V_{OC,Module}$ , which is the open-circuit voltage of the individual PV module. Let  $N_i$  denote the number of the shaded modules with the irradiation not higher than  $G_{Shaded,i}$ , Equation (17) at the  $i$ th turning point  $V_{TP,i}$  is rewritten as (18).

$$V_{TP,i} = (N_{String} - N_i) \times V_{OC,Module} + N_i \times (-V_{BD}) \quad (18)$$

where  $-V_{BD}$  is the breakdown voltage of the shaded modules. However, the value of  $V_{Insolated}$  is closer to  $V_{TP,i}/N_{Insolated}$ , which is smaller than  $V_{OC,Module}$ . The gap between  $V_{TP,i}/N_{Insolated}$  and  $V_{OC,Module}$  cannot be omitted under some shading patterns. As a result, a fractional factor  $\alpha_i$  is proposed in this research to improve the accuracy of the model. The new model is as shown in (19).

$$V_{TP,i} = (N_{String} - N_i) \times \alpha_i V_{OC,Module} + N_i \times (-V_{BD}) \quad (19)$$

In (19), the breakdown voltage  $V_{BD}$  is much smaller than the voltage at turning point  $V_{TP,i}$ . Thus, the value of  $\alpha_i$  can be approximately calculated by letting  $V_{BD} = 0$  and the expression of  $\alpha_i$  is given in (20).

$$\alpha_i = V_{TP,i} / [(N_{String} - N_i) \times V_{OC,Module}] \quad (20)$$

The denominator of (20) is also the first integer multiples

of  $V_{OC,String}/N_{String}$  right to the current  $i$ th turning point. According to (6) and (8), Equation (20) can be rewritten as in (21).

$$\alpha_i = V_{TP,i} / \left[ \frac{V_{OC,String}}{N_{String}} \text{ceil} \left( \frac{N_{String}}{V_{OC,String}} V_{TP,i} \right) \right] \quad (21)$$

Thus, Equation (22) represents the number of shaded modules with their irradiation not higher than  $G_{Shaded,i}$ .

$$N_i = \frac{\alpha_i V_{OC,String} - V_{TP,i}}{\alpha_i V_{OC,Module} + V_{BD}} \quad (22)$$

For a PV string with  $M$  irradiation levels, the index  $i$  in  $N_i$  is from 1 to  $M - 1$ . For simplicity, let  $N_M = 0$ , then the number of shaded modules with the  $i$ th shaded irradiance  $N_{Shaded,i}$  can be expressed as in (23).

$$N_{Shaded,i} = N_i - N_{i+1} \quad (23)$$

Finally, by substituting (23) into (11), the shading rate information can be estimated by (24).

$$\chi_i = \frac{N_i - N_{i+1}}{N_{String}} \quad (24)$$

After the turning points are located by the searching method, the shading strength information and the shading rate information in the shading matrix can be respectively estimated by (28) and (24).

## 2) Estimating the Shading Strength Information

The I-V curve of a PV string under PSC is merged by I-V curves of individual PV modules across the voltage from the higher irradiance to the lower irradiance [27]. Therefore, the current at the  $i$ th turning point, denoted as  $I_{TP,i}$ , approximately equals to the  $i$ th shaded short-circuit current  $I_{SC,Shaded,i}$  as shown in (25).

$$I_{TP,i} \approx I_{SC,Shaded,i} \quad (25)$$

By substituting (13) into (25),  $I_{TP,i}$  can be expressed by (26).

$$I_{TP,i} = (I_{SC,STC} + K_1 \Delta T) \frac{G_{Shaded,i}}{G_{STC}} \quad (26)$$

Similarly, the string short-circuit current  $I_{SC,String}$  is the short-circuit current of the insulated modules  $I_{SC,Insolated}$  as expressed in (27).

$$I_{SC,String} = I_{SC,Insolated} = (I_{SC,STC} + K_1 \Delta T) \frac{G_{Insolated}}{G_{STC}} \quad (27)$$

By substituting (26) and (27) into (10), the shading strength information  $\rho_i$  can be estimated by (28).

$$\rho_i = \frac{I_{TP,i}}{I_{SC,String}} \quad (28)$$

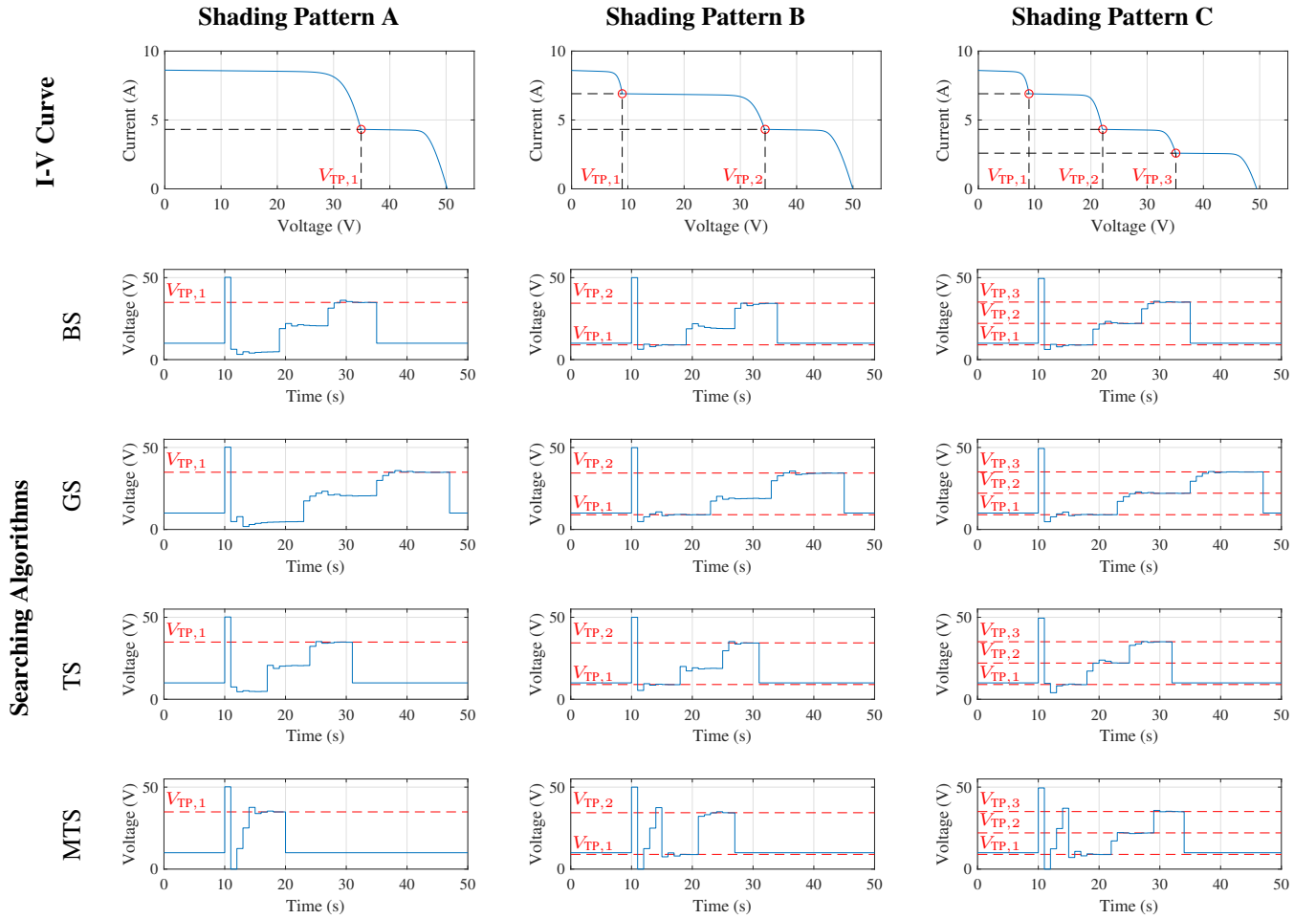


**FIGURE 6.** Comparison in the tracking traces from different searching algorithms under varied shading patterns (shading pattern A: {500,1000,1000,1000}W/m<sup>2</sup>, 25°C; shading pattern B: {500,800,800,1000}W/m<sup>2</sup>, 25°C; shading pattern C: {500,800,300,1000}W/m<sup>2</sup>, 25°C.).

#### IV. RESULTS AND DISCUSSIONS

The proposed shading identification method was validated using simulations in MATLAB/Simulink and experiments with the PV emulator. The specifications of the PV module under STC used in both the simulations and experiments are given in TABLE 1.

##### A. SIMULATION RESULTS

The simulations were conducted using MATLAB/Simulink 2018a. To validate the performance of the proposed identification method, the PV strings with a varied number of modules from 3 to 5 were involved in the simulations. The simulations analyzed the following two aspects:

- 1) The verification of the proposed analytical expressions for the shading matrix by the dataset generated through the simulations.
- 2) The analyses of the proposed MTS-based method for the turning points compared with the basic TS-based method and two other classical searching algorithms: the binary search (BS) algorithm and the golden-

section search (GS) algorithm.

A dataset was generated in Simulink to analyze the accuracy of the proposed analytical expressions for the shading matrix. All the possible shading patterns were involved in the dataset over the temperature range from 0 to 50 °C. The shading strength information and shading rate information in the shading matrix were separately evaluated by three mathematical indicators including root mean squared error (RMSE), mean absolute error (MAE) and R squared (R<sup>2</sup>). Since the dimension of the shading matrix varies from different shading patterns, one estimation's results are split into multiple records in the dataset according to the dimension of the shading matrix. Hence, each record of the dataset only contains one shading strength information and one shading rate information.

The estimation results based on the three mathematical indicators are recorded in TABLE 2. The size of the dataset  $N_{\text{Dataset}}$  is also included. According to the results in TABLE 2, the proposed analytical expression for the shading matrix has a low RMSE value of around 5e-4 when esti-

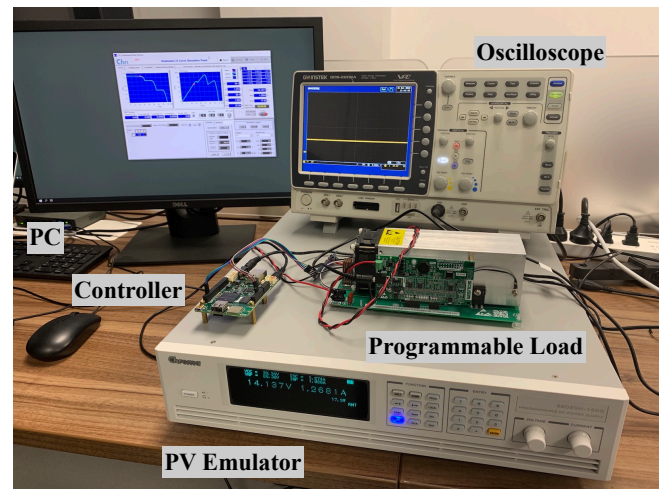
**TABLE 1.** Specifications of the PV module used in this research under standard test conditions.

Parameters	Variable	Value
Short-circuit current	$I_{SC}$	1.22 A
Open-circuit voltage	$V_{OC}$	10.71 V
Current at MPP	$I_{MPP}$	1.12 A
Voltage at MPP	$V_{MPP}$	9.00 V
Maximum power	$P_{MPP}$	10.00 W
Temperature co-efficient of $I_{SC}$	$K_I$	0.062 A/K
Temperature co-efficient of $V_{OC}$	$K_V$	-0.080 V/K

mating the shading strength information. However, the error of the estimated shading strength information is becoming larger with the increase of the string length  $N_{String}$ . The accuracy of the estimated shading rate information is stable and not influenced by  $N_{String}$ .

In order to validate the efficiency of the proposed identification method based on an MTS algorithm, the other three searching algorithms including BS, GS and TS are involved in the comparison study. FIGURE 6 shows the comparison results of the searching tracks for a PV string with four modules under three different shading patterns from the three searching algorithms. The solar irradiations of the four PV modules for the three selected shading patterns are  $\{500,1000,1000,1000\}W/m^2$ ,  $\{500,800,800,1000\}W/m^2$ , and  $\{500,800,300,1000\}W/m^2$  respectively. The temperature is 25 °C. The red horizontal dashed lines represent the position of the turning points. The searching step is 1 s for all three algorithms. Before activating the searching algorithms, the operating voltage is 10 V. All the tests start with measuring the  $V_{OC}$  at the time of 10 s. All the turning points are searched and the searching process finishes when the voltage drops back to 10 V. The same judging criterion and termination condition ( $L_T = 0.1$  V) are used for the three algorithms. As can be seen from the results of the shading pattern A and B, unnecessary searching is observed in the tracks from the identification method based on the BS, GS and TS algorithms. However, with the assistance of the preselection processing of the Tabu intervals, the proposed MTS-based identification method is capable of skipping those intervals which do not contain the turning point. In the shading pattern C when the number of the turning points reaches the maximum, the proposed MTS-based method does not skip any interval but still exhibits a fast searching due to its randomness.

TABLE 3 lists the comparative number of searching steps from the different searching algorithms. Because the random processes exist in the TS-based method and the proposed MTS-based method, the results for the two methods are based on the statistics from 100 runs. The searching rate of the BS, GS and TS algorithms is not affected by the shading pattern but mainly influenced by the number of series modules  $N_{String}$ . However, the performance of the proposed MTS algorithm is largely affected by the shading pattern. With the number of solar irradiation levels increasing, the

**FIGURE 7.** Experimental setup.

average searching step of the proposed algorithm becomes larger. According to the average searching step for different  $N_{String}$ , the proposed MTS algorithm saves at least 18.75% of the searching time and is the most efficient one among the four searching algorithms.

## B. EXPERIMENTAL RESULTS

The experiments in this paper were conducted with the PV emulator (Chroma 62020H-150S) as the shading pattern can be easily configured using this PV emulator. The experimental setup is as shown in FIGURE 7. The computer connected to the PV emulator displays the software panel for the emulator. The programmable load (Sousim 300W) works in the constant voltage mode for adjusting the operating voltage of the PV emulator. The controller board (UDOO NEO) executes the identification algorithms and controls the programmable load through serial communication. The oscilloscope (GW Instek GDS-2202A) records the searching traces.

FIGURE 8 shows the voltage traces recorded by the oscilloscope when tracking the turning points under three different shading patterns labeled from 1 to 3. The solar irradiations for the three shading patterns are  $\{1000,600,400,200\}W/m^2$  (shading pattern 1),  $\{800,500,1000,1000\}W/m^2$  (shading pattern 2) and  $\{800,800,400,400\}W/m^2$  (shading pattern 3). The temperature for the three shading patterns is 25 °C. The PV characteristics curves of each shading pattern are depicted at the top-right corner. The three shading patterns respectively have 3, 2 and 1 turning points. The termination interval length  $L_T$  is set to 0.2 V in the experiments. According to the specifications of the PV module, the reference current difference is 0.061 A.

The PV string is initially operating at the voltage of 10 V. When starting searching, the identification algorithm obtains the string open-circuit voltage  $V_{OC,String}$  by disabling the programmable load. The current values at each  $V_{OC,String}/N_{String}$

**TABLE 2.** Results of the proposed estimation method for the PV strings with different numbers of modules.

N <sub>String</sub>	N <sub>Dataset</sub>	Shading Strength Information			Shading Rate Information		
		RMSE	MAE	R <sup>2</sup>	RMSE	MAE	R <sup>2</sup>
3	418	3.769e-4	2.826e-4	1.0000	0.0123	0.0116	0.9924
4	1122	3.996e-4	2.931e-4	1.0000	0.0120	0.0108	0.9946
5	1980	8.122e-4	3.638e-4	1.0000	0.0116	0.0101	0.9953

**TABLE 3.** Comparison in searching step numbers for varied string lengths from 3 to 5 by different searching algorithms (the results of TS and MTS are based on the statistics of 100 runs).

N <sub>String</sub>	Shading Pattern	BS	GS	TS			MTS		
				Min.	Avg.	Max.	Min.	Avg.	Max.
3	{1000,1000,600}W/m <sup>2</sup> , 25 °C	16	24	15	18	22	8	11	17
	{800,400,400}W/m <sup>2</sup> , 25 °C	16	22	14	17	21	8	11	17
	{1000,300,600}W/m <sup>2</sup> , 25 °C	16	22	12	17	21	14	18	23
	<b>Average</b>	16	23	/	17	/	/	13	/
4	{1000,1000,800,800}W/m <sup>2</sup> , 25 °C	24	34	23	27	33	9	13	17
	{900,600,600,400}W/m <sup>2</sup> , 25 °C	24	34	22	26	31	15	21	29
	{1000,600,200,400}W/m <sup>2</sup> , 25 °C	23	36	21	25	30	22	26	32
	<b>Average</b>	24	35	/	26	/	/	17	/
5	{1000,1000,600,600,600}W/m <sup>2</sup> , 25 °C	32	46	29	35	43	10	13	19
	{1000,1000,1000,400,800}W/m <sup>2</sup> , 25 °C	32	48	28	35	42	16	22	30
	{800,600,400,200,200}W/m <sup>2</sup> , 25 °C	31	44	28	36	44	23	31	40
	<b>Average</b>	32	46	/	35	/	/	22	/

interval boundaries are measured to determine the initial candidate intervals with the turning points. The measuring step is around 1.5 s at the preselection stage. The searching step is around twice the step in the preselection stage since at each step, two voltage points are measured to acquire the slope information. The turning points are correctly located in all the three situations when the voltage drops back to 10 V. On average, it takes 7 steps to search for each turning point. The mean absolute error for the shading strength information in the identified shading matrix is 0.008. The shading rate information is all correctly identified.

**V. CONCLUSIONS**

In this paper, a new form of the shading information called the shading matrix has been introduced to quantitatively analyze the complex PSC with multiple solar irradiation levels. A comprehensive shading identification approach based on an MTS algorithm and analytical models has been proposed to estimate the value of the shading matrix. Simulations and experiments have been conducted to validate the efficiency and effectiveness of the proposed identification method. By comparing with the BS, GS and TS algorithms, the results have shown that the proposed identification method would perceive the shading matrix at least 18.75% faster. In the future, the proposed identification method will be used to instruct the MPPT systems for tracking the GMPP under PSC.

**REFERENCES**

[1] A. Mäki and S. Valkealahti, "Power losses in long string and parallel-connected short strings of series-connected silicon-based photovoltaic

modules due to partial shading conditions," *IEEE Trans. Energy Convers.*, vol. 27, no. 1, pp. 173–183, March 2012.

[2] A. E. Brooks, D. Cormode, A. D. Cronin, and E. Kam-Lum, "PV system power loss and module damage due to partial shade and bypass diode failure depend on cell behavior in reverse bias," in *Proc. IEEE 42nd Photovoltaic Spec. Conf.*, New Orleans, LA, USA, June 2015, pp. 1–6.

[3] Z. Alqaisi and Y. Mahmoud, "Comprehensive study of partially shaded pv modules with overlapping diodes," *IEEE Access*, vol. 7, pp. 172 665–172 675, 2019.

[4] F. Zhang, J. Li, C. Feng, and Y. Wu, "In-depth investigation of effects of partial shading on PV array characteristics," in *Proc. IEEE Power Eng. Autom. Conf.*, Wuhan, China, Sep. 2012, pp. 1–4.

[5] M. Davarifar, A. Rabhi, A. Hajjaji, E. Kamal, and Z. Daneshifar, "Partial shading fault diagnosis in PV system with discrete wavelet transform (DWT)," in *Proc. Int. Conf. Renewable Energy Res. Appl.*, Milwaukee, WI, USA, Oct 2014, pp. 810–814.

[6] K. Hu, S. Cao, W. Li, and F. Zhu, "An improved particle swarm optimization algorithm suitable for photovoltaic power tracking under partial shading conditions," *IEEE Access*, vol. 7, pp. 143 217–143 232, 2019.

[7] J. C. Teo, R. H. G. Tan, V. H. Mok, V. K. Ramachandaramurthy, and C. Tan, "Impact of partial shading on the P-V characteristics and the maximum power of a photovoltaic string," *Energies*, vol. 11, no. 7, 2018.

[8] S. Sarikh, M. Raoufi, A. Bennouna, A. Benlarabi, and B. Ikken, "Fault diagnosis in a photovoltaic system through I-V characteristics analysis," in *Proc. 9th Int. Renew. Energy Congr.*, Hammamet, Tunisia, March 2018, pp. 1–6.

[9] S. S. Kumar and A. I. Selvakumar, "Detection of the faults in the photovoltaic array under normal and partial shading conditions," in *Proc. Innov. Power Adv. Comput. Technol.*, Vellore, India, April 2017, pp. 1–5.

[10] Q. Zhao, S. Shao, L. Lu, X. Liu, and H. Zhu, "A new PV array fault diagnosis method using fuzzy c-mean clustering and fuzzy membership algorithm," *Energies*, vol. 11, no. 1, 2018.

[11] J. Huang, R. Wai, and W. Gao, "Newly-designed fault diagnostic method for solar photovoltaic generation system based on IV-curve measurement," *IEEE Access*, vol. 7, pp. 70 919–70 932, 2019.

[12] S. Fadhel, C. Delpha, D. Diallo, I. Bahri, A. Migan, M. Trabelsi, and M. Mimouni, "PV shading fault detection and classification based on I-V curve using principal component analysis: Application to isolated PV system," *Sol. Energy*, vol. 179, pp. 1–10, 2019.

[13] A. K. Tripathi, M. Aruna, and C. S. N. Murthy, "Performance of a PV

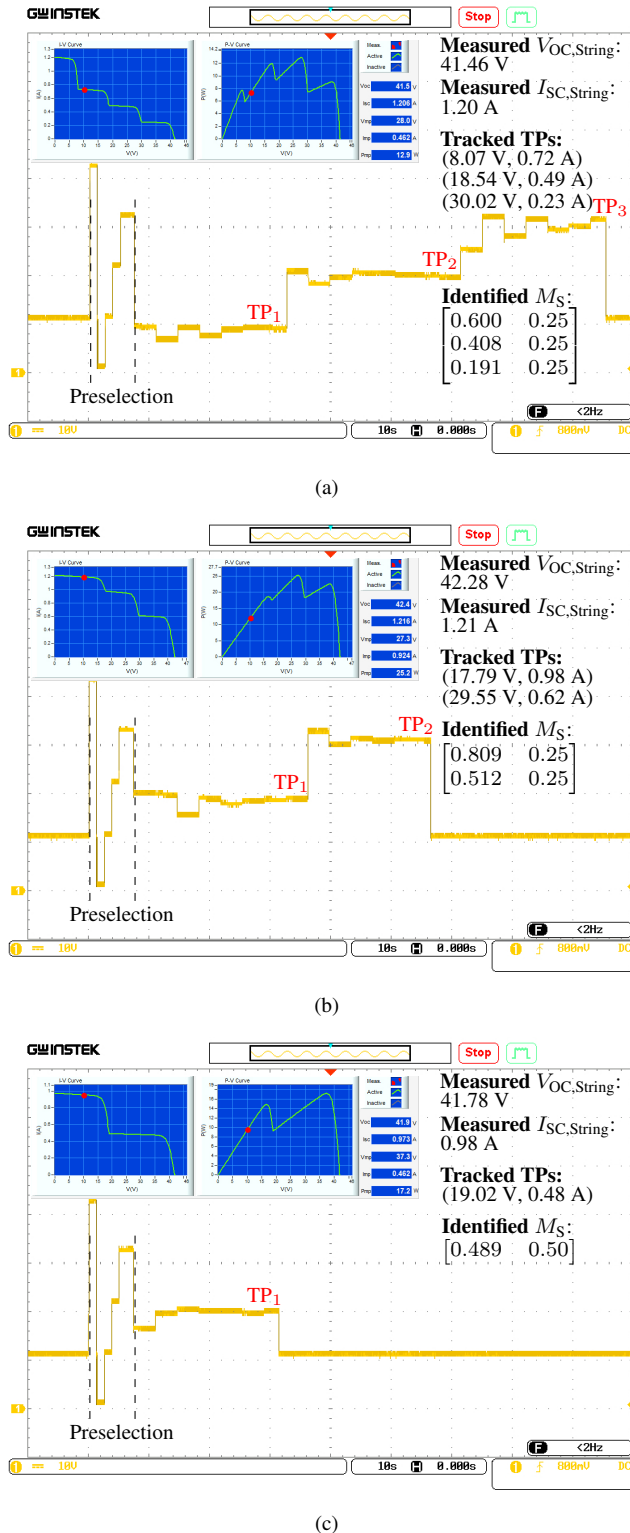


**FIGURE 8.** The tracked voltage traces recorded by the oscilloscope when searching the turning points for a PV string with four PV modules under (a) shading pattern 1:  $\{1000, 600, 400, 200\} \text{W/m}^2$ ,  $25^\circ\text{C}$ ; (b) shading pattern 2:  $\{800, 500, 1000, 1000\} \text{W/m}^2$ ,  $25^\circ\text{C}$  and (c) shading pattern 3:  $\{800, 800, 400, 400\} \text{W/m}^2$ ,  $25^\circ\text{C}$ .

panel under different shading strengths,” *Int. J. Ambient Energy*, vol. 40, no. 3, pp. 248–253, 2019.

[14] J. Ma, X. Pan, K. L. Man, X. Li, H. Wen, and T. On Ting, “Detection and assessment of partial shading scenarios on photovoltaic strings,” *IEEE Trans. Ind. Appl.*, vol. 54, no. 6, pp. 6279–6289, Nov 2018.

[15] F. Salem and M. A. Awadallah, “Detection and assessment of partial shading in photovoltaic arrays,” *J. Electr. Syst. Inf. Technol.*, vol. 3, no. 1, pp. 23–32, 2016.

[16] J. Ma, Z. Bi, K. L. Man, H. Liang, and J. S. Smith, “Predicting the global maximum power point locus using shading information,” in *Proc. 19th IEEE Int. Conf. on Environ. Elect. Eng., 3rd IEEE Ind. Commercial Power Syst. Eur.*, Genova, Italy, June 2019, pp. 1–5.

[17] Z. Bi, J. Ma, K. L. Man, J. S. Smith, Y. Yue, and H. Wen, “Global MPPT method for photovoltaic systems operating under partial shading conditions using the  $0.8V_{oc}$  model,” in *Proc. 19th IEEE Int. Conf. on Environ. Elect. Eng., 3rd IEEE Ind. Commercial Power Syst. Eur.*, Genova, Italy, June 2019, pp. 1–6.

[18] J. Ma, Z. Bi, K. L. Man, Y. Yue, and J. S. Smith, “Automatic shading detection system for photovoltaic strings,” in *Proc. Int. SoC Design Conf.*, Daegu, Korea (South), Nov 2018, pp. 176–177.

[19] L. Davies, R. Thornton, P. Hudson, and B. Ray, “Automatic detection and characterization of partial shading in PV system,” in *Proc. IEEE 7th World Conf. Photovolt. Energy Convers.*, Waikoloa Village, HI, USA, June 2018, pp. 1185–1187.

[20] P. Lei, Y. Li, and J. E. Seem, “Sequential ESC-based global MPPT control for photovoltaic array with variable shading,” *IEEE Trans. Sustain. Energy*, vol. 2, no. 3, pp. 348–358, July 2011.

[21] Young-Hyok Ji, Jun-Gu Kim, S. Park, Jae-Hyung Kim, and Chung-Yuen Won, “C-language based PV array simulation technique considering effects of partial shading,” in *Proc. IEEE Int. Conf. Ind. Technol.*, Gippsland, VIC, Australia, Feb 2009, pp. 1–6.

[22] M. G. Villalva, J. R. Gazoli, and E. R. Filho, “Comprehensive approach to modeling and simulation of photovoltaic arrays,” *IEEE Trans. Power Electron.*, vol. 24, no. 5, pp. 1198–1208, May 2009.

[23] J. Ma, Z. Bi, T. O. Ting, S. Hao, and W. Hao, “Comparative performance on photovoltaic model parameter identification via bio-inspired algorithms,” *Sol. Energy*, vol. 132, pp. 606–616, 2016.

[24] J.-C. Wang, Y.-L. Su, J.-C. Shieh, and J.-A. Jiang, “High-accuracy maximum power point estimation for photovoltaic arrays,” *Sol. Energy Mater. Sol. Cells*, vol. 95, no. 3, pp. 843–851, 2011.

[25] F. Glover, “Tabu search: A tutorial,” *Interfaces*, vol. 20, no. 4, pp. 74–94, 1990.

[26] F. Glover and E. Taillard, “A user’s guide to tabu search,” *Annals of operations research*, vol. 41, no. 1, pp. 1–28, 1993.

[27] X. Li, H. Wen, Y. Hu, L. Jiang, and W. Xiao, “Modified beta algorithm for GMPPT and partial shading detection in photovoltaic systems,” *IEEE Trans. Power Electron.*, vol. 33, no. 3, pp. 2172–2186, March 2018.



ZIQIANG BI (S’19) received the B.Eng. degree in electrical and information engineering from the Suzhou University of Science and Technology, Suzhou, China, in 2016. He is currently working toward the Ph.D. degree with the University of Liverpool, Liverpool, U.K. His current research interests include machine learning and photovoltaic power systems.



**JIEMING MA** (M'15) received the M.Sc. degree in advanced microelectronic systems engineering from the University of Bristol, Bristol, U.K., in 2010, and the Ph.D. degree in computer science from the University of Liverpool, Liverpool, U.K., in 2014.

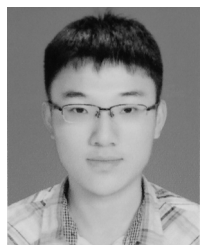
From 2015 to 2017, he was a Lecturer with the Suzhou University of Science and Technology, China. He is currently a Lecturer with the Xi'an Jiaotong-Liverpool University, Suzhou, China. His research interests include intelligent optimization, machine learning, and applications in renewable energy systems.



**YONG YUE** received the B.Sc. degree from Northeastern University, Shenyang, China, and the Ph.D. degree from Heriot-Watt University, Edinburgh, U.K.

He worked in industry for 8 years followed experience in academia with the University of Nottingham, Cardiff University and the University of Bedfordshire, U.K. He is currently a Professor and Director of the Virtual Engineering Centre, Xi'an Jiaotong-Liverpool University, Suzhou, China. His current research interests include computer graphics, virtual reality and robot navigation.

...



**KANGSHI WANG** received his M.Sc. degree in electrical engineering with excellence from the University of New South Wales, Australia, in 2019. From 2019 to 2020, he was a research assistant with the Xi'an Jiaotong-Liverpool University, Suzhou, China. He is currently working towards his Ph.D. in computer science with the University of Liverpool, Liverpool, U.K. His research interests include optimization, machine learning, and FPGA implementations of intelligent control

systems.



**KA LOK MAN** received the Dr.Eng. in Electronic Engineering from Politecnico di Torino, Italy, in 1998, and the Ph.D. degree in Computer Science from Technische University Eindhoven, Netherland, in 2006. He is currently a professor in Computer Science and Software Engineering in Xi'an Jiaotong-Liverpool University, Suzhou, China. His research interests include formal methods and process algebras, embaded system design and testing, and photovoltaics.



**JEREMY S. SMITH** received the B.Eng. (Hons.) degree in engineering science and the Ph.D. degree in electrical engineering from the University of Liverpool, Liverpool, U.K., in 1984 and 1990, respectively.

Between 1984 and 1988, he was conducting research on image processing and robotic systems in the Department of Electrical Engineering and Electronics, University of Liverpool, Liverpool, U.K. He has worked as a Lecturer, Senior Lecturer, and Reader in the same department since 1988. He has held a Professorship since 2006 in electrical engineering at the University of Liverpool. His research interests include automated welding, robotics, vision systems, adaptive control, and embedded computer systems.